Changes in Void Content and Free Volume in Fibers during Heat Setting and Their Influence on Dye Diffusion and Mechanical Properties

N. S. MURTHY, A. C. REIMSCHUESSEL, and V. KRAMER, *Corporate Technology, Allied-Signal Inc., Morristown, New Jersey 07960*

Synopsis

The contributions of the changes in porosity and free volume to the differences in the properties of dry and wet heat set fibers are analyzed. Nylon 6 fibers heat set in wet atmosphere (autoclave and Superba process) show a significantly higher small-angle X-ray scattering intensity between 0.5° and 1.5° (Cu Kα) relative to corresponding non-heat-set fibers, whereas the fibers heat set in dry atmosphere (Suessen process) do not. This scattering arises from the electron density contrast due to pores and free volume which lower the electron density between the fibrils. The average diameter of the crystalline fibrils, as calculated from the Guinier analysis of diffuse scattering, increases from ca. 50 to 65 Å in all fibers upon heat setting. Additional scattering at much lower angles is attributed to aggregates of fibrils. Transmission electron microscopic studies of fibers stained by AgI, through I_2/methanol/$AgNO_3$ treatment, suggest that as AgI crystallizes in a dendritic network along the paths opened up by the diffusion of iodine, it brings about large structural changes in the polymer; this process reveals defects and latent diffusion paths in the fiber. The dendritic structures of AgI are more extensive in wet heat set fibers than in dry heat set and non-heat-set fibers. The ordering within the crystalline domains, the interlamellar spacing, and the density of the fiber increase during both wet and dry processes. The role of these changes in the structure and the morphology of the fibers on the dyeing and ozone fading behavior, and on the strength and the modulus of the fibers, are discussed.

INTRODUCTION

Fibers used in home-furnishings are heat-set to stabilize the twist and crimp so that the yarns maintain the aesthetic appeal of unmatted texture, tuft definition, and resilience during wear. Dye diffusion in fibers is sensitive to the heat setting process. While nylon fibers heat set (annealed) in the presence of moisture (the continuous Superba process and the batch autoclave method, both using saturated steam) dye darker, the fibers heat set in essentially dry atmosphere (the continuous Suessen process) usually dye lighter than the non-heat-set yarns. Analysis by wide- and small-angle X-ray methods has shown that changes in the crystalline and interlamellar regions in both classes of fibers (the wet and the dry process) are similar[1]: Lamellar spacing, crystallite size in the equatorial plane, crystalline and fiber density, and the chain-axis repeat all increase with annealing temperature; this is accompanied by loss of crystalline orientation and a decrease in the van der Waals separation of the hydrogen-bonded sheets. If dye diffusion were to be determined by these parameters alone, then there should be a consistent decrease in the dyeability in both the wet and the dry heat-set fibers.[1] This is contrary to the observations

Journal of Applied Polymer Science, Vol. 40, 249–262 (1990)
 CCC 0021-8995/90/1-20249-14$04.00

cited above. Therefore, the differences in the dyeability of fibers heat-set by different processes should be due to the changes in the amorphous domains, or the porosity of the fibers.[2] Irrespective of which morphological feature affects the diffusion of dyes, wet-heat setting enhances the dye uptake, and therefore yields fibers with a more "open" structure.

In this report, using small-angle X-ray scattering (SAXS) and transmission electron microscopy (TEM), we show that this "open" structure can be attributed to a decrease in the average density of the amorphous matrix between the fibrils caused by an increase in the volume fraction of pores (voids) or by an increase in the free volume. We will use our data to understand the contribution of voids and free volume to the differences in the dye diffusion, ozone fading, and the mechanical properties in the non-heat-set and the heat-set fibers.

EXPERIMENTAL

SAXS data were collected from Suessen, Superba, and autoclave fibers listed in Table I. Control, non-heat set fibers were also analyzed in each case. The data were obtained using a linear proportional counter mounted on a Franks camera.[3] The intensity data were collected along the equator to eliminate the interference from the lamellar peak in the analysis of the equatorial diffuse scattering. The background scattering, obtained with no sample in the beam, was subtracted from the sample curves. The curves were not smoothed. The data were not desmeared since our scattering geometry could be approximated by point collimation. The difference curves were analyzed using the Guinier approximation. No corrections were made for multiple scattering.

The fibers used for electron microscopy were stained with AgI by soaking the fibers in a solution of iodine in methanol, followed by conversion of iodine to AgI by immersing the fibers in an aqueous solution of silver nitrate. The fibers were then washed with distilled water, dried, embedded in epoxy, and sectioned at room temperature for examination in a Hitachi 800 electron microscope operated at 200 kV.

TABLE I

Fiber	Processing mode	Typical heat-setting conditions	Approximate duration (min)
Suessen	Continuous	Dry heat (180–220°C) at atmospheric pressure	1
Superba	Continuous	Saturated steam (110–150°C) at high pressure (75 psig)	1
Autoclave	Batch	Alternate cycles of high pressure (30–35 psig) saturated steam (110–150°C) and vacuum	30

RESULTS

The background subtracted SAXS curves from the Suessen, Superba, and the Autoclave processes are shown in Figure 1 (full lines) along with the scattering curves from the corresponding non-heat-set or control fibers (points). The scattering from the three control fibers are different, and the scattering from heat-set fibers should be compared with the scattering from the corresponding non-heat-set fibers. The left panel (curves a, c, and e) shows the scattering along the fiber axis, and the right panel (curves b, d, and f) shows the scattering perpendicular to the fiber axis. The data in the left panel show

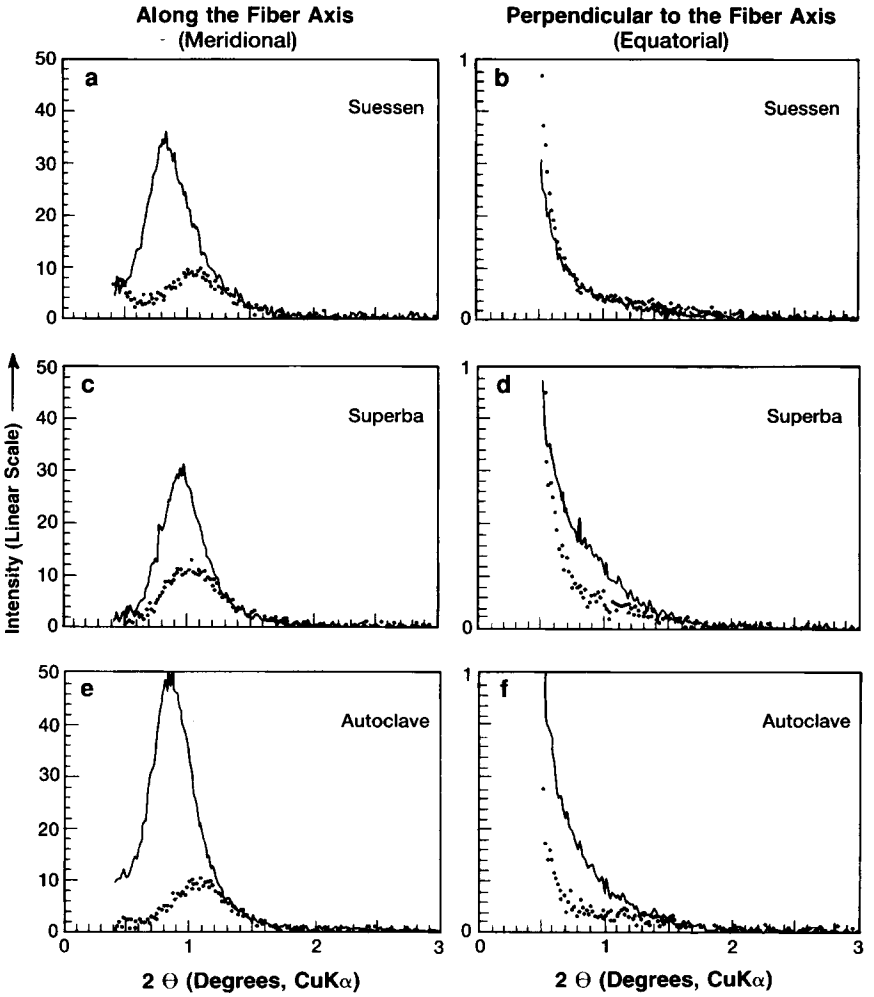

Fig. 1. Small-angle X-ray scattering curves from control (dotted) and heat set (full-line) fibers. Curves in the left panel provide information about lamellae, and the curves in the right panel contain information about fibrils: (a, b) Suessen process; (c, d) Superba process; (e, f) Autoclave process.

that the separation between the lamellae, and the intensity of this lamellar peak, increase upon annealing in all the three classes of fibers (Fig. 2). These increases in lamellar spacing and SAXS intensity can be attributed to the growth of the lamellae and an increase in their crystalline order (see Ref. 1 and references therein). Since the position and intensity of the SAXS peak are sensitive to heat-setting temperature, they can be effectively used to monitor all the three heat-setting processes. In the remainder of the paper, we will concentrate only on the data in the right panel in Figure 1 (curves b, d, and f). This equatorial scattering will be simply referred to as scattering.

The scattering falls off more rapidly in non-heat-set and Suessen-set fibers than in Superba-set and autoclaved fibers (Fig. 1, right panel). This rate of decrease in small-angle diffuse scattering can be analyzed using the Guinier plots ($\ln I(h)$ vs. h^2) shown in Figure 3. Although the Guinier approximation [eq. (1)] is derived for low concentrations of scattering particles, it has been shown[4] that eq. (1) can be used even in concentrated systems, such as dense solids, when the particles are not of uniform size and shape. It can be seen, especially in the non-heat-set and the dry-heat-set fibers, that the Guinier plots

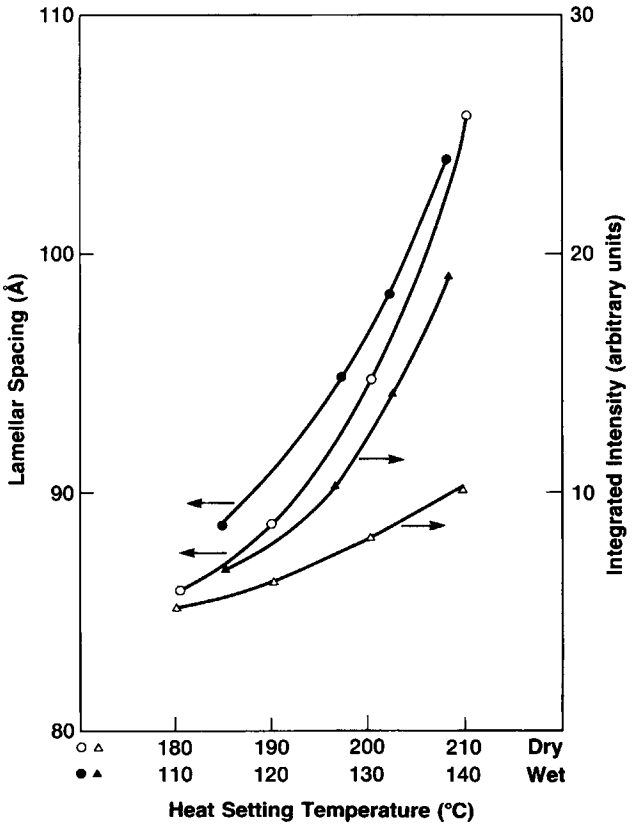

Fig. 2. A plot of the lamellar spacing and SAXS peak intensity as a function of annealing temperature in dry heat set (Suessen) and wet heat set (Autoclave) fibers.

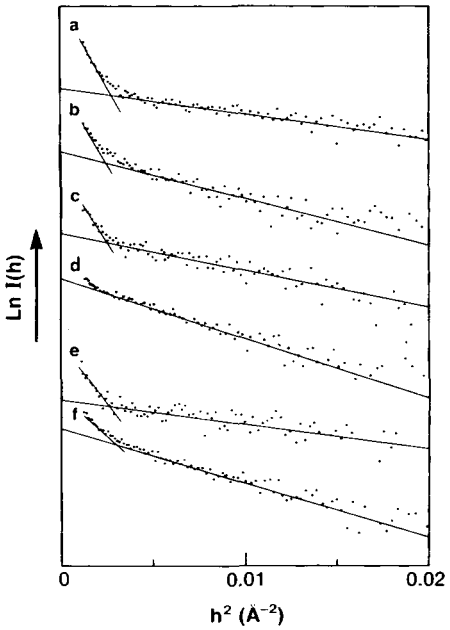

Fig. 3. Guinier plots of the scattering curves shown in Figure 1 (right panel). The curves have been offset vertically for clarity. The curves a, c, and e are from control fibers, and curves b, d and f are from corresponding fibers which are heat set by respectively, Suessen, Superba, and autoclave process.

can be resolved into two straight lines corresponding to scattering from entities of two different sizes. These sizes can be estimated from the relation

$$I(h) = I(0) \exp(-h^2 r^2/5) \tag{1}$$

where $h = (4\pi \sin \theta)/\lambda$, λ is the wavelength (1.542 Å), θ is half the scattering angle, and r is the radius of the circular cross section of an elongated particle whose long axis is normal to the incident X-ray beam.[5]

The results of the Guinier analysis for each of the fibers analyzed are shown in Table II. The slope of the Guinier plots at $h^2 > 0.0075 \text{Å}^{-2}$ corresponds to a diameter d of ca. 50 Å in control fibers, and increases to ca. 65 Å for heat-set fibers. Similar values were obtained in two other sets of experiments. Note that the scattering intensity in this angular range is higher in the wet-heat-set fibers than in the non-heat-set and the dry-heat-set fibers. We will later argue (see Discussion) that this increased scattering is due to higher void content and increased free volume in wet-heat-set fibers, but the size calculated from this scattering is related to the diameter of the fibrils.

We studied a phenol treated fiber to determine the source of the scattering at $2\theta > 1.2°$. A fiber (the non-heat-set fiber in the autoclave series) was immersed in an aqueous 3.5% phenol for 16 h, washed in water for 2 h, and dried. A SAXS scan from this partially dried fiber (Fig. 4) shows a resolvable peak at 1.4° corresponding to a Bragg spacing D of 65 Å. In other phenol-treated fibers,

TABLE II
Estimated Sizes from the Guinier Plots of Control and Heat Set Fibers

	Diameter (Å)	
	Control	Heat-set
$2\theta > 1.2°$, $h^2 > 0.0075$ Å^{-2} [a]		
Suessen	44	57
Superba	57	70
Autoclave	47	65
$2\theta < 1°$, $h^2 < 0.005$ Å^{-2} [b]		
Suessen	145	139
Superba	137	—
Autoclave	139	114

[a] These values correspond to the diameter of the individual fibrils.

[b] These sizes are tentatively assigned to fibrillar aggregates, but may in fact have contributions from other sources such as large pores. These values are probably only lower limits since data in Figure 2 may not extend to sufficiently low angles.

spacings as high as 100 Å were observed. This interference peak can be attributed to periodic fluctuations in electron density between the crystalline fibrils and interfibrillar amorphous regions. The distance D of 65–100 Å is larger than the diameter d of 45–70 Å determined from the Guinier analysis of the slope at $h^2 > 0.005$ Å^{-2} from control and heat set fibers, respectively. This suggests that the diameter d refers to the size of the fibrils, and the distance D might correspond to the interfibrillar separation. These results are illustrated with a model in Figure 5.

As already noted, besides the scattering at $2\theta > 1.2°$, which we have used to calculate the sizes of the fibrils, an additional scattering is present at $2\theta < 1.2°$ in all fibers, suggesting the presence of a second scattering species (Fig. 1). From the limited range of the Guinier plots ($h^2 < 0.005 A^{-2}$), we estimate the lower limit for the diameter of these species to be ca. 150 Å (Fig. 3). This

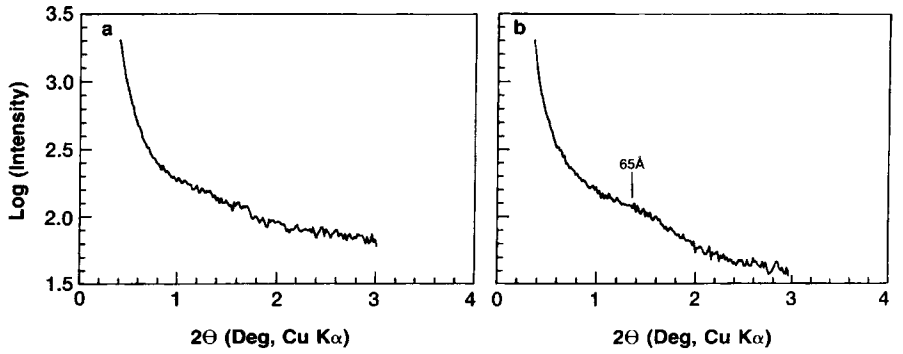

Fig. 4. Comparison of the observed scattering curves for fibers which are: (a) non-heat-set; (b) partially dried after treating with phenol.

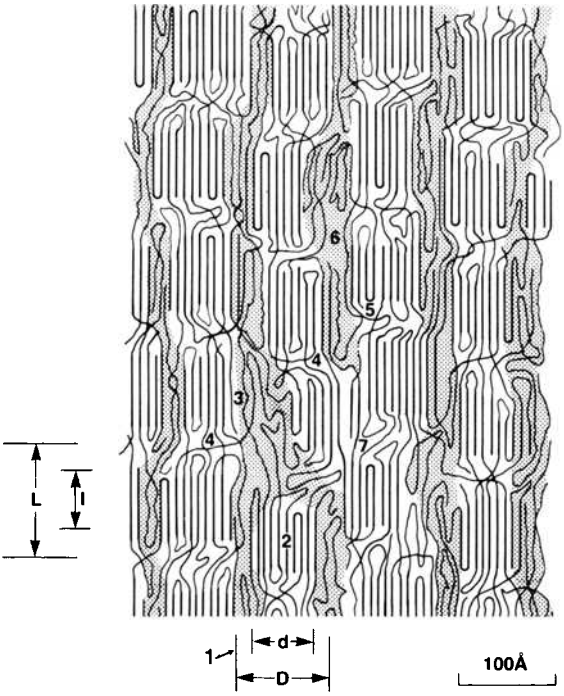

Fig. 5. A model of a filament of nylon 6 to interpret the SAXS and WAXD data in terms of fibrillar crystalline and interfibrillar amorphous regions: (1) fibrils; (2) lamellae; (3) partially extended chains in the interfibrillar regions; (4) tie molecules in the interlamellar region; (5) free chain ends; (6) amorphous segments with large free volume and which may give rise to voids; (7) fusion of adjacent microfibrils.[6] Shaded areas represent the interfibrillar amorphous regions.

scattering essentially remains unchanged during heat setting, and we tentatively attribute this scattering to aggregates of fibrils. Such aggregates have in fact been observed in transmission electron micrographs.[6]

Figure 6 shows transmission electron micrographs of the non-heat-set fibers and the fibers heat-set by Suessen [Figs. 6(a) and (b)], Superba [Figs. 6(c) and (d)], and the autoclave [Figs. 6(e) and (f)] processes. The micrographs show AgI stains formed during the I_2/methanol/$AgNO_3$ treatment. A thin surface layer (0.5 μm) on the fibers remains unstained due to the presence of a dense, oriented skin on the surface of the fiber. The core of the fiber also remains unstained, and this is most likely because the stain cannot diffuse through the already stained outer layers in the cross section of the fiber. The stained regions in the cross sections of the fibers show AgI crystallizing in the form of dendrites. We estimate the size of AgI crystals to be ca. 100 Å (30–150 Å, Fig. 7), and this is in agreement with the value calculated from the line widths in the wide-angle X-ray diffraction (WAXD) scans of the AgI stained fibers. While the degree of staining is lower in Suessen set fibers than in the corresponding control, the autoclave fibers stain more heavily than the corresponding controls. The staining characteristics of the Superba set fibers were somewhat similar to that of the autoclave fibers, except that the staining in

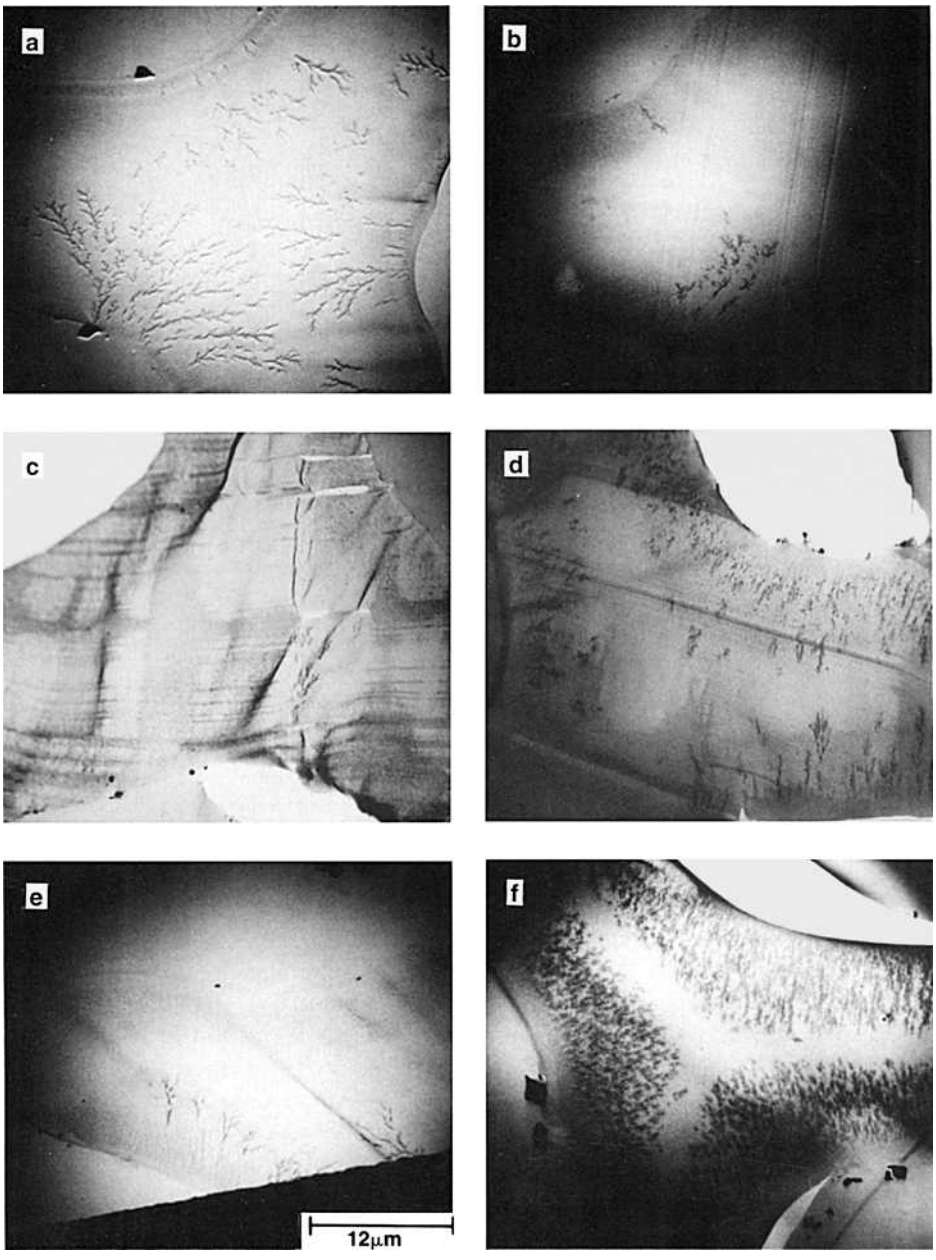

Fig. 6. Transmission electron micrographs of cross sections of AgI stained fibers. Control fibers are shown in the left panel and heat set fibers are shown in the right panel: (a, b) Suessen process; (c, d) Superba process; (e, f) autoclave process.

the Superba set fibers was not consistently heavier than in the corresponding controls. Analysis of 15 sections of control fibers and 16 sections of Superba-set fibers showed that the fractions of fully stained, partially stained, and un-

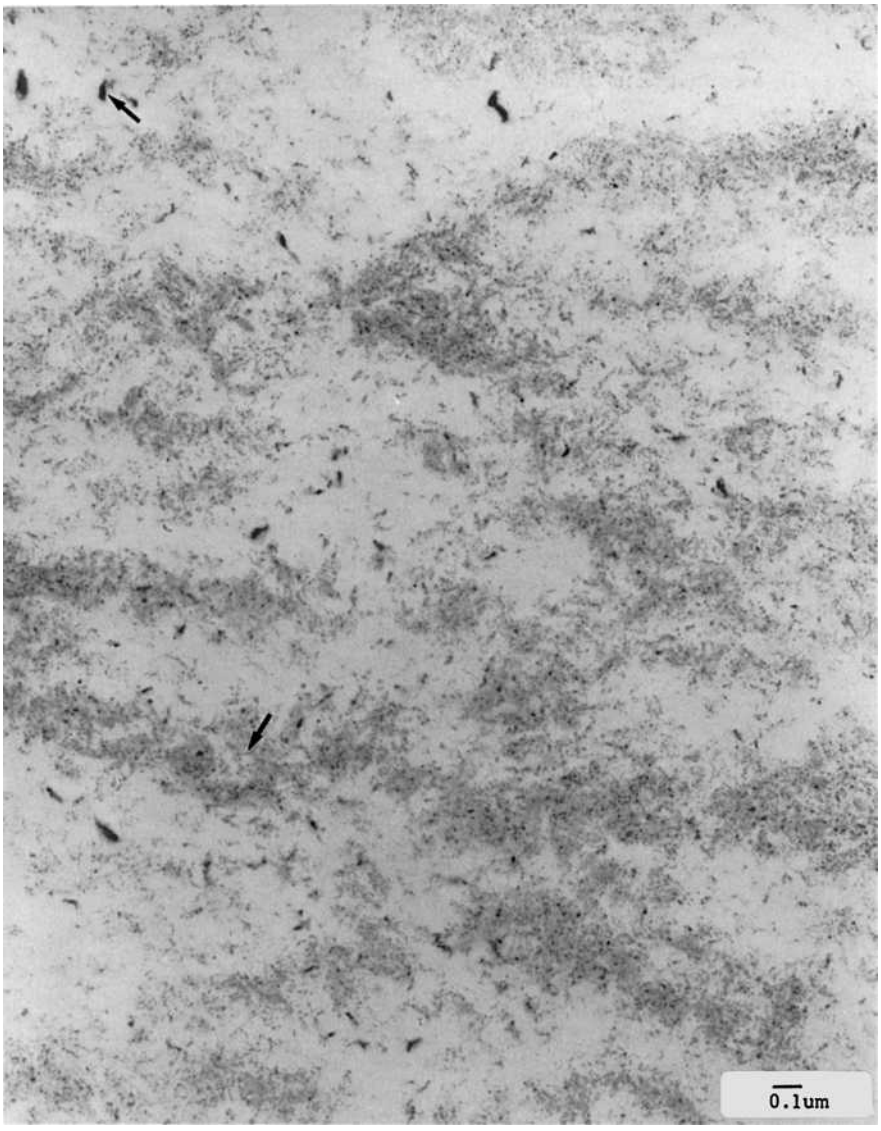

Fig. 7. Transmission electron micrographs of a cross-section of a heat set fiber (autoclave process) after AgI staining and at a magnification higher than in Figure 6(f). In this photograph, smallest dots represent ~ 30 Å size AgI crystals, slightly larger dots are ~ 150 Å AgI crystals, big dark clusters (arrow at the top left-hand corner) are aggregates of AgI crystals, and the small unstained circular areas (arrow at the lower-half of the picture) are aggregates of fibrils.

stained sections were, respectively, 25, 35, and 40% in control fibers, and 70, 20, and 10% in heat-set fibers. These results show that, in general, the degree of staining is higher in Superba- and autoclave-set fibers relative to non-heat-set and Suessen-set fibers. Phenol-treated fibers showed a similar increase in AgI stains relative to the untreated fibers.

DISCUSSION

We will attempt here to interpret the changes in SAXS curves and the different degree of AgI staining in terms of a model which can be used in understanding diffusion and mechanical behavior of fibers. Two models are commonly used, the pore and the free volume models.[2] The pore model describes amorphous regions as a two-phase system made of polymer chains and the voids. The free volume model describes amorphous regions as a single phase system in which the segmental mobility of the chains, rather than voids, influences the dye diffusion. Although diffusion is sometimes interpreted in terms of either a pore model or a free volume model, it is likely that the distinction is in part due to the probe used for measurement, and that diffusion, depending upon whether it occurs above or below the glass transition temperature, is influenced by free volume as well as porosity. SAXS, being sensitive only to average electron density over distances of nanometers, cannot easily distinguish between these two models. The average electron density of the amorphous regions can decrease both due to pores and free volume, and we will use the two terms interchangeably. In the literature, this SAXS scattering along the equator is referred to as void scattering.

Effect of Pores and Free Volume on Diffuse Scattering

Statton[7,8] and Hermans et al.[9] have done extensive work on the changes in the SAXS diffuse scattering that occur during processing of polymer fibers, and attribute the scattering in the equatorial plane to voids. In contrast, in agreement with the work of Heyn,[10] our data suggest that the equatorial small-angle scattering at $h \geq 0.1$ Å^{-1} is due to fibrils. This distinction may not be important, except when determining the sizes, since the scattering according to either interpretation is essentially due to the contrast between the fibrils and the amorphous chain segments laterally separating the fibrils. We suggest that although the intensity of the scattered X-ray can be influenced by the void content, the distribution of this intensity as a function of scattering angle, i.e., the shape of the scattering curve, is determined by the size of the fibrils.

The size of the fibrils, determined by the Guinier analysis of SAXS data, increases from ~50 to ~65 Å upon annealing in both dry and wet-heat-set fibers (Table II). We have seen earlier[1] that the crystallite size, as determined from wide-angle X-ray equatorial reflections, also increases from 50 to 75 Å along the a-axis upon annealing (the increase along the c-axis could not be reliably determined because of the overlapping peaks). This supports our contention that the size determined from the diffuse equatorial scattering using the Guinier analysis refers to the diameter of the fibrils. The size we have calculated for the fibrils is perhaps an average of the crystallite sizes in the equatorial plane.

It has been shown that the increase in the density of the crystalline regions is about the same in the wet- and the dry-heat-set fibers.[1] Therefore, the increase in the contrast and the accompanying higher small-angle intensity in wet-heat-set fibers should be due to a decrease in the density in the interfibrillar amorphous regions. These low density regions are most likely to be regions in which

a significant fraction of the volume is not occupied by polymer chain segments. In a non-heat-set fiber, these regions may be occupied by gases entrapped during spinning. Furthermore, as the moisture introduced during the wet-heat-setting process leaves the fiber, it can leave behind voids and thus increase the free volume available for mobile chain segments. Our results and analyses are consistent with both pore and free volume models, as both pores and enhanced segmental mobility lower the average amorphous density and thus give rise to excess SAXS intensity.

The AgI stains in the electron micrographs show enhancement of any defects already present in the fibers. It is known that iodine forms chemical complexes with nylon 6.[11] Although iodine could change the morphology of the polymer, the diffusion path of iodine could still be regarded as regions most accessible to iodine and methanol, and hence least dense. Unlike I/KI treatment, the I_2/methanol/$AgNO_3$ treatment does not produce the gamma form of nylon 6, and the fiber remains in the alpha form. However, as AgI crystallizes along the path opened up by the diffusion of iodine and methanol, it can bring about large structural changes in the morphology of nylon 6. Thus, AgI dendrites indicate regions which are least dense, and which are most susceptible to crack propagation. A higher concentration of AgI stained areas in wet-heat-set fibers reflects a more "open" structure than in dry-heat-set fibers. The lower limit of 30 Å for the size of the AgI crystals measured in electron micrographs (Fig. 7), is the same as that derived from SAXS and WAXD data (Fig. 5). This is consistent with the proposition that iodine in methanol, as well as dye molecules, diffuse through the interfibrillar regions. An increase in the porosity or free volume in these regions contributes to higher rates of diffusion.

Gas adsorption measurements showed that the surface area increased only in autoclaved fibers (0.41–0.60 m^2/g), and was essentially the same in Suessen and Superba fibers (0.43 and 0.30 m^2/g, respectively). Since these values represent the contribution to the surface area from only those pores which are open to the surface, the higher surface area found in autoclaved fibers suggests an increase in latent cracks, defects, or voids near the surface of the filament. This is consistent with the considerable increase in AgI stains in autoclaved fibers. The more open structure in autoclaved fibers is seen in SAXS as lower average density of the amorphous material in the lateral space between the fibrils as compared with that in non-heat-set and dry-heat-set fibers.

Influence of Heat Setting on Porosity and Free Volume

The increase in small-angle diffuse scattering is observed only in wet-heat-set fibers and not in fibers heat-set in dry atmosphere. Statton[8] reported that in dry and dispersion spun fibers, dry, high temperature heat treatment reduced the amount of diffuse scattering. Wet processing of these fibers, on the other hand, did not show any collapse of the voids. Statton also reported that the effect of after-treatments was negligible in melt-spun fibers. Our data from Suessen-set fibers, which show little change in the diffuse scattering, is consistent with Statton's conclusion. However, in contrast with the findings of Statton, we show that after-treatments, such as wet heat setting, can have a significant effect on the SAXS curves even in melt-spun fibers. More impor-

tantly, our SAXS data show that wet processing of melt-spun fibers leads to increased electron density contrast, and higher SAXS diffuse scattering. We suggest that lower amorphous density resulting from increases in voids and free volume contribute to the higher electron density contrasts.

Both the Superba and the autoclave processes use saturated steam, and are usually referred to as wet processes; in contrast, the Suessen process is a dry heat setting process (Table I). The crystalline regions become more ordered after heat setting in both the wet and the dry methods,[1] but the volume fraction of pores increases only in the wet-heat-set fibers. The marginal decrease in the volume fraction of the pores in dry heat set fibers is likely due to the partial melting and recrystallization of nylon 6 at the high heat setting temperatures. It is possible that in wet-heat-set fibers the moisture diffusing into the fibers occupies a finite volume, thereby swelling the fiber, and when the moisture leaves the fiber upon drying, more free volume becomes available for the mobile chain segments, i.e., the moisture leaves behind microvoids or pores in the amorphous matrix by a process similar to the action of a foaming agent. Partial hydrolysis of the nylon 6 chains in the presence of moisture could also contribute to the increase in the void content. It is quite possible that the pores enhance the mobility of the amorphous chain segments. The pores are probably occupied by neighboring amorphous chain segments for only a fraction of the time during the random thermal fluctuations from the equilibrium positions of these chain segments. Therefore, the voids could decrease the density in the interfibrillar region, and thus enhancing the SAXS intensity due to fibrils.

Influence of Heat Setting on Diffusion and Mechanical Properties

Some of the physical properties of a fiber can be understood in terms of its morphology, i.e., by the distribution of crystalline fibrils, the amorphous regions, and the void content. At low levels of crystallinity, the crystalline regions can undergo large changes (such as increase in crystallinity), and thus influence the properties of the fiber. As the crystallinity approaches a limiting value, other factors such as density and orientation of the amorphous domains, and defects such as voids, significantly affect the properties of the fiber.[1] Although these various factors, as well as other parameters such as glass transition temperature, crystalline perfection, crystallite size, and amorphous and crystalline orientation, can directly or indirectly affect the physical properties of a fiber, we here focus only on the role of the voids and free volume.

Dye diffusion decreases in dry-heat-set fibers probably not so much by the increase in the crystalline perfection as it is by the decrease in the void content. The observed increase in the volume fraction of the voids in Superba and autoclove fibers might directly contribute to an increase in the dye diffusion. Thus, wet processing yields fibers which dye darker and faster. Our data suggest that the increase in the dye uptake in fibers treated with aqueous solutions of benzyl alcohol, phenol, and formic acid is due to an increase in the void content as proposed by Subramanian et al.[12] In contrast, Moore and Weigmann[13] attribute increased dye uptake to greater segmental mobility. As discussed earlier, the presence of pores might increase the free volume and enhance the segmental mobility of the chains in the amorphous regions.

The changes in the void content can be used to interpret some of the data on ozone fading in nylon fibers. Ozone fading is a phenomenon in which, at high humidities, atmospheric ozone appears to oxidize the dyes, thus fading the fibers. Haylock and Rusch[14] noted that dyes which have the least mobility in the fiber are most resistant to ozone fading: that acid dyes (which react with the amine end-groups) desorb from nylon 6 at a much slower rate, and are more ozone resistant than disperse dyes; and that premetallized dyes, which do not desorb significantly into water at 35°C, offer the most resistance to ozone fading. Although such differences in resistance to ozone fading might arise in part from the inherent differences in the resistance of the dyes to degradation by ozone, to explain the generally observed correlation between dye diffusion and the fading of the dyes in humid atmosphere in the presence of ozone, Haylock and Rusch suggested that dye molecules are destroyed at the surface of the fibers once they diffuse out from the interior of the fiber. But microspectrophotometric studies of dye diffusion by Kamath, Ruetsch, and Weigmann[15] suggest that ozone penetration into the fiber substantially contributes to the fading process. One cannot, however, completely discount the hypothesis of Haylock and Rusch, since it is possible that the reactivity of ozone may decrease rapidly as it diffuses into the fiber. Whatever may be the diffusing entities, dyestuff or ozone, fading is higher in humid atmospheres and in wet-heat-set fibers. In view of our data on the void content, the increase in the rate of fading of dyes due to atmospheric ozone in a humid atmosphere, and the independently observed increased rate of dye diffusion in steam-heat-set fibers, can now be attributed to the increase in free volume or the volume fraction of the voids which offer least resistance to the diffusion of the dyes and ozone.

The observed differences in the free volume or the void content can also be used to understand the differences in the mechanical properties of the fibers after dry and steam heat setting.[16] It was noted that, although the crystallinity and the density were higher in steam-heat-set fibers, the increase in the Young's modulus in steam-heat-set fibers was not as large as in dry-heat-set fibers. It is possible to explain these apparently incompatible results by invoking the role of the increased void content in the steam-heat-set fibers, and by the increase in the number of latent cracks, defects or voids near the surface of the filament. These changes can also account for the decrease in the tensile strength of the fibers in steam-heat-set fibers, and a corresponding increase in dry-heat-set fibers, relative to non-heat-set fibers.

CONCLUSION

Heat-setting (annealing) nylon 6 fibers in a moist atmosphere results in fibers with higher void content or free volume. This contributes to increase in the dye uptake and decrease in the tensile strength of the fibers.

We thank Dr. A. J. Signorelli for valuable suggestions throughout this work, Mr. J. L. Rush for discussions on heat setting and dyeing, and for providing some of the fibers, Drs. K. Zero and M. E. McDonnell for porosity measurements and for reviewing the manuscript, Drs. W. Hammond and R. A. F. Moore for their valuable comments, and Professor S. Krimm for frequent discussions.

References

1. N. S. Murthy, H. Minor, and R. A. Latif, *J. Macromol. Sci. Phys.*, **B26,** 427–446 (1987).
2. R. M. Rohner and H. Zollinger, *Text. Res. J.*, **56,** 1–13 (1986).
3. N. S. Murthy, *Norelco Rep.*, **30,** 35–39 (1983).
4. A. Guinier and G. Fournet, *Small-Angle X-Ray Scattering,* Wiley, New York, 1955 pp. 70, 187.
5. A. Guinier and G. Fournet, *Small-Angle X-Ray Scattering,* Wiley, New York, 1955, p. 134.
6. A. C. Reimschuessel and D. C. Prevorsek, *J. Polym. Sci. Polym. Phys. Ed.*, **14,** 485–498 (1976).
7. W. O. Statton, *J. Polym. Sci.*, **22,** 387–397 (1956).
8. W. O. Statton, *J. Polym. Sci.*, **56,** 205–220 (1962).
9. P. H. Hermans, D. Heikens, and A. Weidinger, *J. Polym. Sci.*, **35,** 145–165 (1959).
10. A. N. J. Heyn, *Text. Res. J.*, **23,** 782–787 (1953).
11. N. S. Murthy, *Macromolecules,* **20,** 309–316 (1987).
12. D. R. Subramanian, A. Venkatataman, and N. V. Bhat, *J. Appl. Polym. Sci.*, **27,** 4149–4159 (1982).
13. R. A. F. Moore and H.-D. Weigmann, *Text. Res. J.*, **56,** 180–190 (1986).
14. J. C. Haylock and J. L. Rush, *Text. Res. J.*, **46,** 1–8 (1976).
15. Y. K. Kamath, S. B. Ruetsch, and H.-D. Weigmann, *Text. Res. J.*, **53,** 391–402 (1983).
16. M. Tsuruta and A. Koshimo, *J. Appl. Polym. Sci.*, **9,** 3–9 (1965).

Received December 27, 1988
Accepted March 20, 1989